

Epigenetic clock detected a breast cancer mitosis subtype with improved immunotherapy

Shipeng Shang

College of Bioinformatics Science and Technology

Xin Li

College of Bioinformatics Science and Technology

Yue Gao

College of Bioinformatics Science and Technology

Shuang Guo

College of Bioinformatics Science and Technology

Hanxiao Zhou

College of Bioinformatics Science and Technology

Dailin Sun

College of Bioinformatics Science and Technology

Hongjia Liu

College of Bioinformatics Science and Technology

Hui Zhi

College of Bioinformatics Science and Technology

Peng Wang

College of Bioinformatics Science and Technology

Jing Bai

College of Bioinformatics Science and Technology

Shangwei Ning (✉ ningsw@ems.hrbmu.edu.cn)

Harbin Medical University

Xia Li

College of Bioinformatics Science and Technology

Research

Keywords: DNA methylation, epigenetic clock, epigenetic age deceleration, breast cancer subtype, immunotherapy

Posted Date: February 18th, 2021

DOI: <https://doi.org/10.21203/rs.3.rs-196073/v1>

License:  This work is licensed under a Creative Commons Attribution 4.0 International License.

[Read Full License](#)

18 **Abstract**

19 **Background**

20 Epigenetic clock based on DNA methylation can estimate the epigenetic age of tissue
21 and cell that can describe the process of aging. However, the exploration of diseases by
22 the epigenetic clock is still an uncharted territory. Our objective was to assess the role
23 of the epigenetic clock in breast cancer.

24 **Methods**

25 In this study, DNA methylation data of breast tissue sample was download from TCGA
26 and GEO database. DNA methylation level of CpG sites and age of samples was
27 calculated by using pearson correlation test. Differentially expressed genes were
28 identified using the limma package and Kruskal-Wallis test was used for the difference
29 between cancer subtypes.

30 **Results**

31 We developed a workflow to construct the Breast Epigenetic Clock (BEpiC) that could
32 accurately predict the chronological age of normal breast tissue. Furthermore, the
33 BEpiC was applied to breast cancer to identify three breast cancer subtypes (including
34 development, homeostasis, and mitosis) by using the deviation between epigenetic age
35 and chronological age. Interestingly, the prognosis of the three breast cancer subtypes
36 is significantly different. In addition, the three breast cancer subtypes had distinct
37 differences in multiple immune cells and the mitosis subtype had the highest tumor
38 mutation burden that was used to estimate response to checkpoint inhibitors.

39 **Conclusion**

40 Our model highlights that epigenetic age of breast cancer samples had an important
41 impact on immunotherapy. We constructed a BEpiC web server ([http://bio-
42 bigdata.hrbmu.edu.cn/BEpiC/](http://bio-bigdata.hrbmu.edu.cn/BEpiC/)) where users submit DNA methylation data and age
43 information to predict the epigenetic age of breast tissue and breast cancer subtypes.

44 **Trial registration**

45 Not applicable

46 **Keywords:** DNA methylation; epigenetic clock; epigenetic age deceleration; breast
47 cancer subtype; immunotherapy

48

49 **Background**

50 DNA methylation is an important epigenetic marker and plays critical roles during
51 mammalian development, including X chromosome inactivation, cell differentiation
52 and parental imprinting(1, 2). DNA methylation, especially methylation of CpG island
53 (CGI), can suppress gene expression(3) and inactivate tumor suppressor genes in
54 human cancers(4). DNA methylation exhibits dynamic changes(5) and are more stable
55 than RNA during aging(6). Therefore, some researchers have built epigenetic clock that
56 can predict human epigenetic age based on methylation levels of multiple human tissues
57 and blood(7-11). However, DNA methylation pattern is specific in human tissues and
58 shows a negative correlation with aging in some tissues(12, 13). A more accurate
59 epigenetic clock needs to be developed for individual tissue. Epigenetic clock was also
60 used to predict the biological age based on the methylation level of multiple tissues in
61 mouse(14). Daniel et al. found that epigenetic clock could be used to evaluate

62 interventions that alter the rate of aging, such as calorie restricted diet(15). In addition,
63 the mitotic clock based on DNA methylation found that the epigenetic age acceleration
64 in normal tissues increases the risk of cancer(16, 17). In brief, epigenetic clock could
65 measure aging of tissues that are independent of chronological age.

66 Cancer is the most common type of malignancy which is currently one of the leading
67 causes of death worldwide(18). The development of cancer has been shown to be
68 associated with global hypomethylation and local hypermethylation(19). Previous
69 studies found that DNA methylation loss in late-replicating partial methylation domains
70 promotes immune evasion of tumors, especially in domains with CGI
71 hypermethylation(20). Hypermethylation in the promoter region of important gene can
72 lead to gene expression disorders that promote cancer(21, 22). DNA methylation occurs
73 at an early stage of cancer, so it plays an important role in cancer screening and
74 prognosis prediction(23, 24). Methylated DNA has been shown to be specific in cancers,
75 so it can be used as a potential tumor marker(25, 26). Breast cancer is a highly
76 heterogeneous cancer with a higher incidence in women. Studies have also found that
77 the increased risk of breast cancer may be associated with DNA methylation of
78 promoter region of BRCA1(27). Aging is associated with molecular, cellular, and
79 physiological changes that affect carcinogenesis and cancer growth(28, 29). Epigenetic
80 clock based on methylation that describes the aging process may be useful for the study
81 of cancer closely related to aging.

82 The response triggered by immunotherapy intervention will clearly target and eliminate
83 tumor cells while retaining normal cells(30). At present challenge facing

84 immunotherapy is selecting biomarkers that predict clinical responses to CTLA-4 and
85 PD-1 blockade. Multiple studies have shown that immunotherapy is associated with
86 breast cancer molecular subtypes that can provide prognostic information for breast
87 cancer patients(31, 32). However, some studies suggested that existing subtypes did not
88 predict treatment effects of patients(33).

89 We developed a breast epigenetic clock to identify cancer subtypes that respond
90 differently to immunotherapy based on the deviation between epigenetic age and
91 chronological age. Eventually, a web server of epigenetic clock constructed based on
92 DNA methylation that was used to calculate the epigenetic age and identify cancer
93 subtypes in breast tissue. Cancer subtypes based on epigenetic clock may provide a
94 theoretical basis for early cancer diagnosis and immunotherapy (Figure1).

95

96 **Methods**

97 **DNA methylation data collection and preparation**

98 DNA methylation datasets of breast cancer based on Illumina Infinium
99 HumanMethylation450 BeadChip array were obtained from the TCGA portal
100 (<http://xena.ucsc.edu/>). We preprocessed DNA methylation data by removing probes
101 that were on the sex chromosomes and chondriosome. In addition, the CpG sites with
102 single nucleotide polymorphism (SNP) and missing value were also removed. Finally,
103 351,427 CpG sites passed quality control. We removed the sample without age
104 information, and the remaining samples contained 788 samples of breast cancer and 96
105 samples of paracancerous tissue. In the follow-up analysis, we considered the

106 paracancerous samples as normal samples.

107 To avoid outlier samples, we used principal component analysis (PCA)(34) for normal
108 samples. Firstly, we calculated the squared distance from the first principal component
109 of each sample to the population mean as the z-score of the sample. Then, we converted
110 z-score(7) to a false-discovery rate using the Gaussian cumulative distribution and the
111 Benjamini-Hochberg procedure.

$$112 \quad Z_i = (PC_i - \frac{1}{n} \sum_i^n PC_i)^2$$

113 Where Z_i

114 Samples with FDR below 0.05 are considered outliers and removed. Finally, four
115 samples were removed.

116 **The construction of breast epigenetic clock (BEpiC)**

117 Initially, correlation coefficient between age and DNA methylation level (beta values)
118 of CpG sites was calculated by using pearson correlation test and multiple testing
119 correction was performed using false discovery rate (FDR). CpG sites with FDR less
120 than 0.05 were defined as significant age-related CpG sites.

121 We randomly divided 92 samples into training set and testing set according to the ratio
122 of 1:1. We constructed the breast epigenetic clock using the elastic-net generalized
123 linear model as implemented in the GLMNET package(35). By using 10-fold cross-
124 validation, optimal lambda (2.296) was identified. Finally, we obtained 21 CpG sites
125 and corresponding weights through elastic regression network. The epigenetic age
126 EpiAge was defined as

127
$$\text{EpiAge} = \left(\sum_i^n w_i * M_i \right) + c$$

128 where w_i is the weight of CpG_i , M_i is the methylation level of CpG_i and $c = -86.729$.

129 Eventually, we then used the validation set and a public dataset which at NCBI Gene

130 Expression Omnibus (GEO) under accession number GSE108213(20) and

131 GSE67919(36) to verify the predict performance of BEpiC.

132 **Genomic enrichment analysis of significant aging-associated CpG sites**

133 To understand the enrichment of aging-associated CpG sites on the genome.

134 Normalized degree of enrichment(14) was calculated as:

135
$$N_i = \left(\frac{s}{b} \times \frac{B}{S} \right) - 1$$

136 Where s , b are the number of significant sites and the number of background sites at a

137 given region i , such as CpG island. S , B is total number of significant sites and total

138 number of background sites, respectively.

139 **Breast cancer subtypes based on epigenetic age**

140 We calculated the epigenetic age of breast cancer samples by using BEpiC. The mean

141 absolute error (MAE) between chronological age and epigenetic age of normal breast

142 sample from TCGA and GSE108213 is 5.3 years. We use twice the MAE (5.3 years) of

143 BEpiC in normal samples as the standard for dividing subtypes. Breast cancer samples

144 were divided into three subtypes, which were samples with deviation between

145 epigenetic age and chronological age higher than 10.6 years, samples with deviation

146 between epigenetic age and chronological age lower than 10.6 years, and the remaining

147 samples. Up-regulated genes for each breast cancer subtype were screened in a “one vs.

148 rest” fashion by using the Bioconductor package limma, with false-discovery rate-

149 corrected p-value less than 0.05 and fold change greater than 1.5 considered significant.

150 **Statistical Analysis**

151 CpG sites that differ in methylation between tumor and normal samples were defined
152 by t test and multiple testing correction was performed using FDR. CpG sites with both
153 FDR<0.05 and a minimum change of ± 0.3 in DNA methylation level between tumor
154 samples and normal samples were defined as differential methylation CpG sites. The
155 Kaplan-Meier survival plots were used to estimate OS and disease-free survival (DFS),
156 and the difference in OS or DFS between the Development, Homeostasis and Mitosis
157 subtype was determined using log-rank tests with R package ‘survival’. The mitotic
158 index could reflect the proportion of dividing cells in the population. Studies have
159 confirmed that the mitotic index can be represented by the average expression level of
160 mRNA of CDKN3, ILF2, KDELR2, RFC4, TOP2A, MCM3, KPNA2, CKS2 and
161 CDC2(16). We used the average FPKM expression values of the nine genes in the
162 cancer samples to represent the mitotic indexes of each sample. To calculate TMB of
163 breast cancer samples, synonymous variant and intron variant was excluded(13).
164 Finally, the number of mutations on the million-base was calculated as the TMB of the
165 sample. Tumor-infiltrating immune cells in breast cancer samples was estimated by
166 CIBERSORT(37). The R package “estimate”(38) was used to evaluate stromal score
167 and immune score of breast cancer sample. All the statistical analyses were performed
168 in R versions 3.5.3.

169 **Results**

170 **DNA methylation is associated with age in human breast tissue**

171 DNA methylation data of 884 breast samples were downloaded from The Cancer
172 Genome Atlas (TCGA) and tissues adjacent to cancer were extracted as normal breast
173 tissues, aged 28 to 90. Aging-associated CpG sites were identified by using Pearson
174 correlation analysis between age and DNA methylation levels of CpG sites in normal
175 breast tissues. 4,330 CpG sites were associated with age, of which 4,150 (95.8%) CpG
176 sites were significantly positively correlated with age (Figure 2A). It shows that DNA
177 methylation levels of most of aging-associated CpG sites increase with age in normal
178 breast tissues (Figure 2B). This phenomenon has also been demonstrated in other
179 human tissues(39). Some CpG sites regulated the expression of age-associated gene
180 (Supplementary Figure 1). It proves that aging-associated DNA methylation may cause
181 gene expression to change with aging.

182 We corrected the number of all probes on each genomic region in Illumina Infinium
183 HumanMethylation450 BeadChip to test the enrichment of aging-related CpG sites on
184 the genomic region. The significantly positive aging-associated CpG sites mainly
185 enriched in CpG island shore, exon and 2Kb downstream regions of the gene. CpG sites
186 which significantly negatively correlated with age mainly enriched in the CpG island
187 desert, introns and intergenic regions. We found that changes of DNA methylation
188 levels of aging-associated CpG sites rarely occur on CpG islands and promoter regions
189 (Figure 2C). It can be inferred that these two regions may protect the DNA methylation
190 levels of aging-associated CpG sites and this phenomenon was also found in multiple
191 tissues of mouse(14). Next, the relationship between aging and cancer in DNA
192 methylation level was explored. We identified 5,192 differential methylation CpG sites

193 (DMC) between breast cancer samples and normal samples. There was significant
194 correlation (cor: -0.4457) between DNA methylation difference level of DMC and
195 aging-correlation coefficient of DMC by pearson correlation test (Figure 2D). This
196 suggested that cancer and aging were opposite processes(40) in breast tissue(12). This
197 phenomenon is also confirmed at the level of gene expression(41). Hypermethylated
198 CpG sites in cancer were demethylated during aging, conversely, Hypomethylated CpG
199 sites in cancer were methylated during aging.

200

201 **Epigenetic clock could predict the chronological age of normal breast tissue**

202 A dataset consisting of 92 normal breast samples and 351427 CpG sites was constructed.
203 The dataset was randomly divided into training set and testing set according to the ratio
204 of 1:1. We used an elastic-net regression model to predict the age of normal breast tissue
205 samples and the final model was based on 21 CpG sites. BEpiC was constructed using
206 the DNA methylation level and weight of 21 CpG sites and performed well across
207 training set and testing set. In training set, epigenetic age is highly correlated with
208 chronological age (cor: 0.9807), with mean absolute error (MAE) is 3.62 years (Figure
209 3A). In testing set, the correlation coefficient between epigenetic age and chronological
210 age is 0.8815, with MAE is 6.10 years (Figure 3B). GSE108213(42) dataset was
211 downloaded from Gene Expression Omnibus (GEO <https://www.ncbi.nlm.nih.gov/geo/>)
212 as an independent validation set, including 85 normal breast samples. Epigenetic age of
213 samples from GSE108213 were calculated by BEpiC and is relevant to chronological
214 age (cor: 0.657), with MAE is 5.77 years (Figure 3C). The weight of 21 CpG sites is

215 closely related to correlation coefficients between DNA methylation level and age
216 (Figure 3D). In addition, the 21 CpG sites are mainly located in the gene body and
217 neighboring genes were enriched in the known functions including DNA replication,
218 mitotic cell cycle and lipid transport.

219 Then, we compared the prediction performance of BEpiC and the Horvath clock for
220 epigenetic age of breast tissues. Epigenetic age identified by BEpiC had significant
221 correlation with that identified by Horvath clock in Dataset1 and GSE108213
222 (Supplementary Figure 2). And MAE between epigenetic age and chronological age
223 from BEpiC and Horvath clock were 4.86 years and 7.59 years in normal breast samples
224 from TCGA, respectively. In GSE108213, MAE between epigenetic age and
225 chronological age from BEpiC and Horvath clock were 5.77 years and 9.60 years,
226 respectively (Figure 3E). GSE67919(36) was also downloaded to compare the
227 predictive performance of BEpiC and Horvath model for epigenetic age of normal
228 breast tissue. The correlation between chronological age and epigenetic age by BEpiC
229 and Horvath was 0.703 and 0.679, respectively (Figure 3F-G). The MAE between
230 epigenetic age and chronological age of BEpiC was significantly less than that of
231 Horvath in GSE67919 (Figure 3H). Thus, BEpiC was more accurate than Horvath clock
232 for predicting epigenetic age for breast normal samples.

233

234 **Epigenetic clock identified three breast cancer subtypes**

235 The DNA methylation pattern of breast cancer samples had changed compared to
236 normal tissue. To test whether epigenetic age could predict the chronological age of

237 breast tumor sample, BEpiC was used to calculate epigenetic age in breast cancer
238 samples. We found a large difference between the epigenetic age and chronological age
239 of breast cancer samples (MAE: 17.55 years). This is because the aging process of
240 breast cancer tissue was significantly different from that of normal tissue(43).

241 It has not yet been determined whether there is heterogeneity in breast cancer tumor
242 samples with different aging patterns. So, breast cancer samples were divided into three
243 subtypes based on the deviation between epigenetic age and chronological age (Figure
244 4A). A sample whose epigenetic age was 10.6 years (twice the MAE of BEpiC in
245 normal samples) older than chronological age was defined as epigenetic age
246 acceleration. Then, a sample whose epigenetic age was 10.6 years younger than
247 chronological age was defined as epigenetic age deceleration. To obtain the biological
248 characteristics of each subtype, we identified genes which were significantly up-
249 regulated in a subtype compared with other subtypes (Figure 4B). High expression
250 genes in the epigenetic age acceleration samples mainly enriched in mammary gland
251 epithelium development, mammary gland epithelial cell proliferation, mammary gland
252 development, branching involved in mammary gland duct morphogenesis and
253 reproductive structure development, so we termed this subtype as development
254 (Supplementary Figure 3A). High expression genes in the epigenetic age deceleration
255 samples mainly enriched in mitotic nuclear division, mitotic spindle assembly, spindle
256 assembly, nuclear division and organelle fission, so we termed this subtype as mitosis
257 (Supplementary Figure 3C). High expression genes in remaining samples mainly
258 enriched in retina homeostasis, antibacterial humoral response, tissue homeostasis,

259 receptor-mediated endocytosis and regulation of respiratory burst, so we termed this
260 subtype as homeostasis (Supplementary Figure 3B).

261 We compared the overall survival and disease-free survival of breast cancer patients
262 with three subtypes (Figure 4C). Patients of these three subtypes have significant
263 differences in overall survival ($p=0.00047$) and disease-free survival (Supplementary
264 Figure 3D). Patients with development subtype had the best prognosis and patients with
265 mitosis subtype had the worst prognosis. We inferred that breast cancer patients whose
266 epigenetic age is decelerated may have worse survival prognosis. Similarly, samples
267 with epigenetic age deceleration were also found to have higher cancer risk in normal
268 colon tissue(44). This may suggest that epigenetic age deceleration is danger signal in
269 both normal and cancer tissues. Mitotic index of breast cancer samples was calculated
270 and negatively correlated with epigenetic age (cor: -0.288). Patients with mitosis
271 subtype had a higher tumor mitotic rate than patients in other subtypes (Figure 4D).
272 This indicates that tumor cells in mitosis subtype were more active than other
273 subtypes(18), so breast cancer patients with mitosis subtype had a worse survival
274 prognosis.

275

276 **Molecular and clinical characteristics analysis of mitosis subtype.**

277 To explain the differences of the three subtypes at survival, we examined the somatic
278 mutation of the three subtypes. TP53 is a tumor suppressor gene, and its mutation occurs
279 in many breast cancer patients(45, 46). In 788 samples, TP53 mutations occurred 223
280 (28.3%) breast cancer samples (Supplementary Figure 4). We found that the mutation

281 frequency of TP53 is lowest in development subtype (24%), the mutation frequency of
282 TP53 is highest in mitosis subtype (32%), and the mutation frequency of TP53 is 28%
283 in homeostasis subtype. TTN that proved to be associated with breast cancer
284 prognosis(47) had different mutation frequency in three subtypes. The mutation
285 frequencies of TTN were 18%, 21% and 31% in development, homeostasis, and mitosis
286 subtype, respectively (Figure 5A-C). Next, copy number variation in breast cancer
287 patients was analyzed. It was found that the three subtypes had significant differences
288 in copy number amplification ($p < 2.2e-16$) and copy number deletion($p = 1.3e-14$). The
289 mitosis subtype was significantly higher than the other two subtypes in terms of copy
290 number amplification and copy number deletion (Figure 5D-E). This may reveal the
291 reasons for the poor survival prognosis of the mitosis subtype.

292 The clinical information of breast cancer patients was obtained from TCGA. The
293 proportion of patients with three subtypes was calculated in stage T, stage N, stage M
294 and pathological stage. It was found that the proportion of patients with mitosis subtype
295 in T4, N3, stage iii-iv was higher than the other two subtypes (Supplementary Table 2).
296 It also demonstrated that most breast cancer patients with mitosis subtype were
297 advanced cancer patients with poor prognosis.

298 We analyzed the relationship between PAM50 signature and BEpiC and found that
299 Basal subtypes has a large overlap with mitosis subtypes (Figure 5F). This indicates
300 that the epigenetic age of breast cancer tissues was decelerate in the Basal subtypes, so
301 the prognosis of Basal subtypes patients was worse.

302

303 **Immunotherapy has a better therapeutic effect for mitotic subtype**

304 We focus on the treatment of patients with three subtypes, and whether the patients with
305 three subtypes are different in terms of medication. We compared the prognosis of three
306 breast cancer subtypes taking tamoxifen as a commonly used drug in the treatment of
307 breast cancer (Supplementary Figure 5). There was no significant difference in
308 prognosis of the three subtypes taking tamoxifen ($p=0.57$).

309 Since the patients of the three subtypes were significantly different at the molecular
310 level and survival prognosis, we wanted to know if the patients of the three subtypes
311 are different for immunotherapy. The proportion of immune infiltrating cells in breast
312 cancer samples was calculated using CIBERSORT (<https://cibersort.stanford.edu/>), and
313 the difference in the proportion of immune infiltrating cells of samples of the three
314 subtypes was compared (Supplementary Figure 6A). Activated T cells CD4 memory, T
315 cells follicular helper, Macrophages M0 and Macrophages M1 differed significantly
316 among the three subtypes and had a higher proportion in mitosis subtype. While naive
317 B cells, plasma cells, resting memory CD4 T cells, resting dendritic cells and resting
318 mast cells differed significantly among the three subtypes and had a lower proportion
319 in mitosis subtype (Figure 6). The different infiltration patterns indicated that the three
320 subtypes might have different immune system.

321

322 Previous studies have shown that stromal cells have a huge impact on immunotherapy
323 (48, 49). Stromal scores of breast cancer samples were evaluated by using R Package
324 “estimate”. Stromal score of mitosis subtype was significantly higher than stromal score

325 of development subtype ($p = 0.011$) and homeostasis subtype ($p = 0.00046$,
326 Supplementary Figure 6B). This may indicate that stromal environment of patients with
327 mitosis subtype is significantly different from the other two subtypes. We also
328 compared the tumor mutation burden among the three subtypes and found that tumor
329 mutation burden (TMB) of patients with mitosis subtypes had significantly higher than
330 the other two subtypes (Figure 7A). Basal subtypes and Her2 subtypes also had higher
331 TMB than the LumA subtypes and LumB subtypes. This proved that Basal subtypes and
332 Her2 subtypes might have a better response to immunotherapy (Supplementary Figure
333 6C). It shows that mitosis subtype had a better immunotherapy response than the other
334 two subtypes(50).

335 Cytotoxic T-lymphocyte-associated protein 4 (CTLA4) is a key immune checkpoint
336 which maintain the immune system(51). Expression level of CTLA4 was compared in
337 three subtypes and significantly different between development subtype and mitosis
338 subtype (Figure 7B). Methylation of CTLA4 can be used to assess response of
339 immunotherapy(52), so we focus on whether expression of CTLA4 is regulated by
340 methylation. Four CpG sites were found in the promoter region of CTLA4 and their
341 methylation levels were lower in the mitosis subtype compared to the development
342 subtype. It suggests difference in methylation of CpG results in difference of expression
343 levels of immune genes and ultimately might affect the response to immunotherapy(53).

344

345 **Online tool for breast epigenetic clock**

346 To help researchers get epigenetic age of breast tissue and breast cancer subtype, we

347 developed a BEpiC web server (<http://bio-bigdata.hrbmu.edu.cn/BEpiC/>). The platform
348 (Figure 8) provides a friendly interface that provides computing and download
349 functions. To obtain the epigenetic age of breast tissue, users need to submit
350 methylation data containing 21 CpG sites. If users want to get the breast cancer subtype,
351 they need to add chronological age information.

352

353 **Discussion**

354 Horvath and Hannum have built epigenetic clock in multiple human tissues and blood(8,
355 14, 54), but DNA methylation exhibits tissue-specific pattern in mammals that regulates
356 tissue-specific gene transcription(55). Therefore, it is necessary to establish a tissue-
357 specific age prediction model, which can more accurately predict the chronological age
358 of tissues. In this study, we systematically examined the associations between age and
359 DNA methylation in breast tissue. BEpiC was constructed to predict epigenetic age
360 significantly associated with chronological age in normal breast tissue. Epigenetic age
361 that can describe the degree of aging was associated with mortality independently of
362 chronological age(44). BEpiC was also used to identify breast cancer subtypes based
363 on the difference between epigenetic age of breast cancer samples and chronological
364 age. The three subtypes had significant differences in prognosis and the mitosis subtype
365 had the worst prognosis. We also found that epigenetic age had a negative correlation
366 with cell mitosis. Epigenetic age deceleration is a risk factor not only for normal
367 tissues(44, 56), but also for cancer tissues. It might confirm that breast tissue tissues
368 with epigenetic age deceleration had higher mitotic index. Mitotic cell division

369 increases tumor mutation burden and copy number variation, making tumor cells easier
370 to recognize by immune cells(28).

371 So, we studied the response to immunotherapy among the three subtypes. The mitosis
372 subtype had higher TMB and it might lead to that mitosis subtype had a better
373 immunotherapy response than the other two subtypes(50).

374 **Conclusions**

375 Using DNA methylation data, we constructed an apparent clock of breast tissue that
376 could be used to classify breast cancer subtypes. Our results suggest that breast cancer
377 samples presenting epigenetic age deceleration had a poor survival prognosis and a
378 better response to immunotherapy. The findings may contribute to the diagnosis and
379 treatment of breast cancer.

380

381 **List of abbreviations**

382 BEpiC: Breast Epigenetic Clock

383 CGI: CpG island

384 TCGA: The Cancer Genome Atlas

385 DMC: Differential methylation CpG sites

386 GEO: Gene Expression Omnibus

387 CIBERSORT: Cell-type Identification By Estimating Relative Subsets Of RNA

388 Transcripts

389 TMB: Tumor mutation burden

390 CTLA-4: Cytotoxic T-lymphocyte-associated protein 4

391 SNP: Single nucleotide polymorphism

392 PCA: Principal component analysis

393 MAE: Mean absolute error

394 FDR: False-discovery rate

395

396 **Declarations**

397 **Ethics approval and consent to participate**

398 Not applicable

399 **Consent for publication**

400 Not applicable

401 **Availability of data and materials**

402 All data relevant to the study are included in the article or as supplementary material.

403 **Competing interests**

404 No potential conflicts of interest were disclosed.

405 **Funding**

406 National Key R&D Program of China [2018YFC2000100]; National Natural Science

407 Foundation of China [32070672, 61873075]; Heilongjiang Touyan Innovation Team

408 Program.

409 **Author's contributions**

410 Xia Li, Shangwei Ning and Jing Bai designed and directed all the research. Shipeng

411 Shang, Xin Li, Gao Yue, Guo Shuang, Hanxiao Zhou, Dailin Sun, Hongjia Liu, Hui

412 Zhi and Peng Wang performed the data processing and experimental

413 analysis. Shipeng Shang, Xin Li and Gao Yue drafted the manuscript. All authors
414 reviewed and approved the final version of the manuscript.

415 **Acknowledgments**

416 This research is based on the data of GDC Data Portal and GEO database. Thanks to
417 all the members of the research group for help of this manuscript.

418

419 **References**

- 420 1. Smith ZD, Meissner A. DNA methylation: roles in mammalian development. *Nat Rev Genet.*
421 2013;14(3):204-20.
- 422 2. Greenberg MVC, Bourc'his D. The diverse roles of DNA methylation in mammalian development
423 and disease. *Nat Rev Mol Cell Biol.* 2019;20(10):590-607.
- 424 3. He XJ, Chen T, Zhu JK. Regulation and function of DNA methylation in plants and animals. *Cell Res.*
425 2011;21(3):442-65.
- 426 4. Levine JJ, Stimson-Crider KM, Vertino PM. Effects of methylation on expression of TMS1/ASC in
427 human breast cancer cells. *Oncogene.* 2003;22(22):3475-88.
- 428 5. Koch CM, Wagner W. Epigenetic-aging-signature to determine age in different tissues. *Aging*
429 (Albany NY). 2011;3(10):1018-27.
- 430 6. Brock MV, Hooker CM, Ota-Machida E, Han Y, Guo M, Ames S, et al. DNA methylation markers and
431 early recurrence in stage I lung cancer. *N Engl J Med.* 2008;358(11):1118-28.
- 432 7. Hannum G, Guinney J, Zhao L, Zhang L, Hughes G, Sada S, et al. Genome-wide methylation profiles
433 reveal quantitative views of human aging rates. *Mol Cell.* 2013;49(2):359-67.
- 434 8. Horvath S. DNA methylation age of human tissues and cell types. *Genome Biol.* 2013;14(10):R115.
- 435 9. Voisin S, Harvey NR, Haupt LM, Griffiths LR, Ashton KJ, Coffey VG, et al. An epigenetic clock for
436 human skeletal muscle. *J Cachexia Sarcopenia Muscle.* 2020;11(4):887-98.
- 437 10. Shireby GL, Davies JP, Francis PT, Burrage J, Walker EM, Neilson GWA, et al. Recalibrating the
438 epigenetic clock: implications for assessing biological age in the human cortex. *Brain.* 2020.
- 439 11. Zhang Q, Vallerga CL, Walker RM, Lin T, Henders AK, Montgomery GW, et al. Improved precision of
440 epigenetic clock estimates across tissues and its implication for biological ageing. *Genome Med.*
441 2019;11(1):54.
- 442 12. Dmitrijeva M, Ossowski S, Serrano L, Schaefer MH. Tissue-specific DNA methylation loss during
443 ageing and carcinogenesis is linked to chromosome structure, replication timing and cell division rates.
444 *Nucleic Acids Res.* 2018;46(14):7022-39.
- 445 13. Dor Y, Cedar H. Principles of DNA methylation and their implications for biology and medicine.
446 *Lancet.* 2018;392(10149):777-86.
- 447 14. Stubbs TM, Bonder MJ, Stark AK, Krueger F, Team BIAC, von Meyenn F, et al. Multi-tissue DNA
448 methylation age predictor in mouse. *Genome Biol.* 2017;18(1):68.
- 449 15. Petkovich DA, Podolskiy DI, Lobanov AV, Lee SG, Miller RA, Gladyshev VN. Using DNA Methylation

450 Profiling to Evaluate Biological Age and Longevity Interventions. *Cell Metab.* 2017;25(4):954-60 e6.

451 16. Yang Z, Wong A, Kuh D, Paul DS, Rakyan VK, Leslie RD, et al. Correlation of an epigenetic mitotic
452 clock with cancer risk. *Genome Biol.* 2016;17(1):205.

453 17. Youn A, Wang S. The MiAge Calculator: a DNA methylation-based mitotic age calculator of human
454 tissue types. *Epigenetics.* 2018;13(2):192-206.

455 18. Collaborators GBDCoD. Global, regional, and national age-sex-specific mortality for 282 causes of
456 death in 195 countries and territories, 1980-2017: a systematic analysis for the Global Burden of Disease
457 Study 2017. *Lancet.* 2018;392(10159):1736-88.

458 19. Shukla V, Coumoul X, Lahusen T, Wang RH, Xu X, Vassilopoulos A, et al. BRCA1 affects global DNA
459 methylation through regulation of DNMT1. *Cell Res.* 2010;20(11):1201-15.

460 20. Jung H, Kim HS, Kim JY, Sun JM, Ahn JS, Ahn MJ, et al. DNA methylation loss promotes immune
461 evasion of tumours with high mutation and copy number load. *Nat Commun.* 2019;10(1):4278.

462 21. Esteller M, Silva JM, Dominguez G, Bonilla F, Matias-Guiu X, Lerma E, et al. Promoter
463 hypermethylation and BRCA1 inactivation in sporadic breast and ovarian tumors. *J Natl Cancer Inst.*
464 2000;92(7):564-9.

465 22. Lee DD, Leao R, Komosa M, Gallo M, Zhang CH, Lipman T, et al. DNA hypermethylation within TERT
466 promoter upregulates TERT expression in cancer. *J Clin Invest.* 2019;129(1):223-9.

467 23. Muller HM, Oberwalder M, Fiegl H, Morandell M, Goebel G, Zitt M, et al. Methylation changes in
468 faecal DNA: a marker for colorectal cancer screening? *Lancet.* 2004;363(9417):1283-5.

469 24. Watanabe Y, Kim HS, Castoro RJ, Chung W, Estecio MR, Kondo K, et al. Sensitive and specific
470 detection of early gastric cancer with DNA methylation analysis of gastric washes. *Gastroenterology.*
471 2009;136(7):2149-58.

472 25. Liu H, Liu X, Zhang S, Lv J, Li S, Shang S, et al. Systematic identification and annotation of human
473 methylation marks based on bisulfite sequencing methylomes reveals distinct roles of cell type-specific
474 hypomethylation in the regulation of cell identity genes. *Nucleic acids research.* 2016;44(1):75-94.

475 26. Chen WD, Han ZJ, Skoletsy J, Olson J, Sah J, Myeroff L, et al. Detection in fecal DNA of colon cancer-
476 specific methylation of the nonexpressed vimentin gene. *J Natl Cancer Inst.* 2005;97(15):1124-32.

477 27. Prajzencanc K, Domagala P, Hybiak J, Rys J, Huzarski T, Szwiec M, et al. BRCA1 promoter
478 methylation in peripheral blood is associated with the risk of triple-negative breast cancer. *Int J Cancer.*
479 2020;146(5):1293-8.

480 28. Balducci L, Ershler WB. Cancer and ageing: a nexus at several levels. *Nat Rev Cancer.* 2005;5(8):655-
481 62.

482 29. Wang Y, Zhang J, Xiao X, Liu H, Wang F, Li S, et al. The identification of age-associated cancer
483 markers by an integrative analysis of dynamic DNA methylation changes. *Sci Rep.* 2016;6:22722.

484 30. Jia H, Truica CI, Wang B, Wang Y, Ren X, Harvey HA, et al. Immunotherapy for triple-negative breast
485 cancer: Existing challenges and exciting prospects. *Drug Resist Updat.* 2017;32:1-15.

486 31. Denkert C, von Minckwitz G, Darb-Esfahani S, Lederer B, Heppner BI, Weber KE, et al. Tumour-
487 infiltrating lymphocytes and prognosis in different subtypes of breast cancer: a pooled analysis of 3771
488 patients treated with neoadjuvant therapy. *The Lancet Oncology.* 2018;19(1):40-50.

489 32. Sorlie T, Perou CM, Tibshirani R, Aas T, Geisler S, Johnsen H, et al. Gene expression patterns of
490 breast carcinomas distinguish tumor subclasses with clinical implications. *Proc Natl Acad Sci U S A.*
491 2001;98(19):10869-74.

492 33. Pogue-Geile KL, Song N, Jeong JH, Gavin PG, Kim SR, Blackmon NL, et al. Intrinsic subtypes, PIK3CA
493 mutation, and the degree of benefit from adjuvant trastuzumab in the NSABP B-31 trial. *J Clin Oncol.*

494 2015;33(12):1340-7.

495 34. Svante, Wold, and, Kim, Esbensen, and, et al. Principal component analysis.

496 35. Friedman J, Hastie T, Tibshirani R. Regularization Paths for Generalized Linear Models via
497 Coordinate Descent. *J Stat Softw.* 2010;33(1):1-22.

498 36. Hair BY, Xu Z, Kirk EL, Harlid S, Sandhu R, Robinson WR, et al. Body mass index associated with
499 genome-wide methylation in breast tissue. *Breast Cancer Res Treat.* 2015;151(2):453-63.

500 37. Newman AM, Liu CL, Green MR, Gentles AJ, Feng W, Xu Y, et al. Robust enumeration of cell subsets
501 from tissue expression profiles. *Nat Methods.* 2015;12(5):453-7.

502 38. Yoshihara K, Shahmoradgoli M, Martinez E, Vegesna R, Kim H, Torres-Garcia W, et al. Inferring
503 tumour purity and stromal and immune cell admixture from expression data. *Nat Commun.*
504 2013;4:2612.

505 39. Perez RF, Tejedor JR, Bayon GF, Fernandez AF, Fraga MF. Distinct chromatin signatures of DNA
506 hypomethylation in aging and cancer. *Aging Cell.* 2018;17(3):e12744.

507 40. Campisi J. Aging, cellular senescence, and cancer. *Annu Rev Physiol.* 2013;75:685-705.

508 41. Chatsirisupachai K, Palmer D, Ferreira S, de Magalhaes JP. A human tissue-specific transcriptomic
509 analysis reveals a complex relationship between aging, cancer, and cellular senescence. *Aging Cell.*
510 2019;18(6):e13041.

511 42. Harlid S, Xu Z, Kirk E, Wilson LE, Troester MA, Taylor JA. Hormone therapy use and breast tissue
512 DNA methylation: analysis of epigenome wide data from the normal breast study. *Epigenetics.*
513 2019;14(2):146-57.

514 43. Calcinotto A, Kohli J, Zagato E, Pellegrini L, Demaria M, Alimonti A. Cellular Senescence: Aging,
515 Cancer, and Injury. *Physiological Reviews.* 2019;99(2):1047-78.

516 44. Wang T, Maden SK, Luebeck GE, Li CI, Newcomb PA, Ulrich CM, et al. Dysfunctional epigenetic aging
517 of the normal colon and colorectal cancer risk. *Clin Epigenetics.* 2020;12(1):5.

518 45. Zhang Y, Xiong S, Liu B, Pant V, Celii F, Chau G, et al. Somatic Trp53 mutations differentially drive
519 breast cancer and evolution of metastases. *Nat Commun.* 2018;9(1):3953.

520 46. Patocs A, Zhang L, Xu Y, Weber F, Caldes T, Mutter GL, et al. Breast-cancer stromal cells with TP53
521 mutations and nodal metastases. *The New England journal of medicine.* 2007;357(25):2543-51.

522 47. Eriksson N, Benton GM, Do CB, Kiefer AK, Mountain JL, Hinds DA, et al. Genetic variants associated
523 with breast size also influence breast cancer risk. *BMC Med Genet.* 2012;13:53.

524 48. Turley SJ, Cremasco V, Astarita JL. Immunological hallmarks of stromal cells in the tumour
525 microenvironment. *Nat Rev Immunol.* 2015;15(11):669-82.

526 49. Mao M, Yu Q, Huang R, Lu Y, Wang Z, Liao L. Stromal score as a prognostic factor in primary gastric
527 cancer and close association with tumor immune microenvironment. *Cancer Med.* 2020;9(14):4980-90.

528 50. Huang RSP, Haberberger J, Severson E, Duncan DL, Hemmerich A, Edgerly C, et al. A pan-cancer
529 analysis of PD-L1 immunohistochemistry and gene amplification, tumor mutation burden and
530 microsatellite instability in 48,782 cases. *Mod Pathol.* 2020.

531 51. Xiaolei L, Wenhui S, Changshun S, Yufang S, Weidong H. Emerging predictors of the response to
532 the blockade of immune checkpoints in cancer therapy. *Cellular & Molecular Immunology.* 2018.

533 52. Goltz D, Gevensleben H, Vogt TJ, Dietrich J, Dietrich D. CTLA4 methylation predicts response to
534 anti-PD-1 and anti-CTLA-4 immunotherapy in melanoma patients. *jci insight.* 2018.

535 53. Goltz D, Gevensleben H, Vogt TJ, Dietrich J, Golletz C, Bootz F, et al. CTLA4 methylation predicts
536 response to anti-PD-1 and anti-CTLA-4 immunotherapy in melanoma patients. *JCI Insight.* 2018;3(13).

537 54. Knight AK, Craig JM, Theda C, Baekvad-Hansen M, Bybjerg-Grauholm J, Hansen CS, et al. An

538 epigenetic clock for gestational age at birth based on blood methylation data. *Genome Biol.*
539 2016;17(1):206.
540 55. Moore LD, Le T, Fan G. DNA methylation and its basic function. *Neuropsychopharmacology.*
541 2013;38(1):23-38.
542 56. McKenna BG, Hendrix CL, Brennan PA, Smith AK, Stowe ZN, Newport DJ, et al. Maternal prenatal
543 depression and epigenetic age deceleration: testing potentially confounding effects of prenatal stress
544 and SSRI use. *Epigenetics.* 2020:1-11.

545

546 **Figures legends**

547 **Figure 1. The Construction and application of breast epigenetic clock.**

548 **Figure 2. Aging-associated CpG sites in normal breast tissue. (A)** Overview of
549 pearson correlation calculated in normal breast tissue. Nominal correlations are
550 highlighted (p value < 0.05) in wathet (positive) and light red (negative). Significant
551 correlations are highlighted (FDR < 0.05) in blue (positive) and red (negative). **(B)**
552 Heatmap of DNA methylation of aging-associated CpG sites. A white to green gradient
553 represents the gradual increase in age. **(C)** Genome enrichment of aging-associated
554 CpG sites (tested using chi-square test; *p value < 0.05). **(D)** Correlation between DNA
555 methylation difference of DMC and aging-correlation coefficient of DMC. The
556 horizontal axis represents the correlation coefficient between age and DNA methylation
557 of DMC in normal samples. The vertical axis represents DNA methylation difference
558 between cancer samples and normal samples.

559 **Figure 3. Chronological age was predicted based on DNA methylation in human**
560 **breast tissue. (A-C)** Epigenetic age vs. chronological age from training set **(A)**, testing
561 set **(B)** and GSE108213 dataset **(C)**. **(D)** Scatter plot depicting the relationship between
562 weight and aging-correlation coefficient of CpG sites. Blue spots are negatively aging-
563 associated CpG sites and orange spots are positively aging-associated CpG sites. **(E)**

564 Comparison of predictive performance between BEpiC and the Horvath clock. The Y-
565 axis represents the mean absolute error between epigenetic age and chronological age
566 (tested using t test; * represent $p < 0.05$, ** represent $p < 0.01$, *** represent $p < 0.001$,
567 **** represent $p < 0.0001$). (F-G) Chronological age vs. epigenetic age estimated by
568 BEpiC (F) and Horvath clock (G) in GSE67919. (H) Comparison of predictive
569 performance between BEpiC and the Horvath clock in GSE67919 (tested using t test;
570 * represent $p < 0.05$, ** represent $p < 0.01$, *** represent $p < 0.001$, **** represent
571 $p < 0.0001$).

572 **Figure 4. Three breast cancer subtypes identified by BEpiC based on epigenetic**
573 **age. (A)** Subtypes of breast cancer were classified based on the deviation between
574 methylated age and chronological age. (B) Gene signature expression profiler and GO
575 annotation for the three subtypes. The red dot, the yellow dot, and the blue dot represent
576 development subtype, homeostasis subtype and mitosis subtype, respectively. (C)
577 Kaplan–Meier curve for patients of the three subtypes. (D) Mitotic index in three
578 subtypes (p values by Wilcoxon test).

579 **Figure 5. Molecular differences among the three subtypes. (A-C)** Gene mutation
580 frequency in development subtype (A), homeostasis subtype (B) and mitosis subtype
581 (C). (D-E) Number of copy number amplification (D) and copy number deletion (E)
582 among the three subtypes (P values by Kruskal-Wallis test). (F) Association between
583 breast cancer subtypes defined by BEpiC and pam50 molecular subtypes.

584 **Figure 6. Immune infiltrating cells that differ significantly between the three**
585 **subtypes. (A-J)** Comparison of proportion of T cell CD4 memory activated, T cell CD4

586 memory resting, T cell follicular helper, Macrophages M0, Macrophages M1, B cells
587 naive, Plasma cells, Dendritic resting, Mast cells resting among the three subtypes (P
588 values by Kruskal-Wallis test).

589 **Figure 7. Comparison of immunotherapeutic response among the three subtypes.**

590 **(A)** Tumor mutation burden in each subtype (P values by Kruskal-Wallis test). **(B)**
591 Expression of CTLA4 in each subtype (P values by Kruskal-Wallis test). **(C-F)**
592 Methylation level of cg05074138 **(C)**, cg08460026 **(D)**, cg22572158 **(E)** and
593 cg26091609 **(F)** in development subtype and mitosis subtype.

594 **Figure 8. Schematic overview of the breast epigenetic clock.** The web server could
595 use the data submitted by the user to calculate the epigenetic age and breast cancer
596 subtypes.

597

Figures

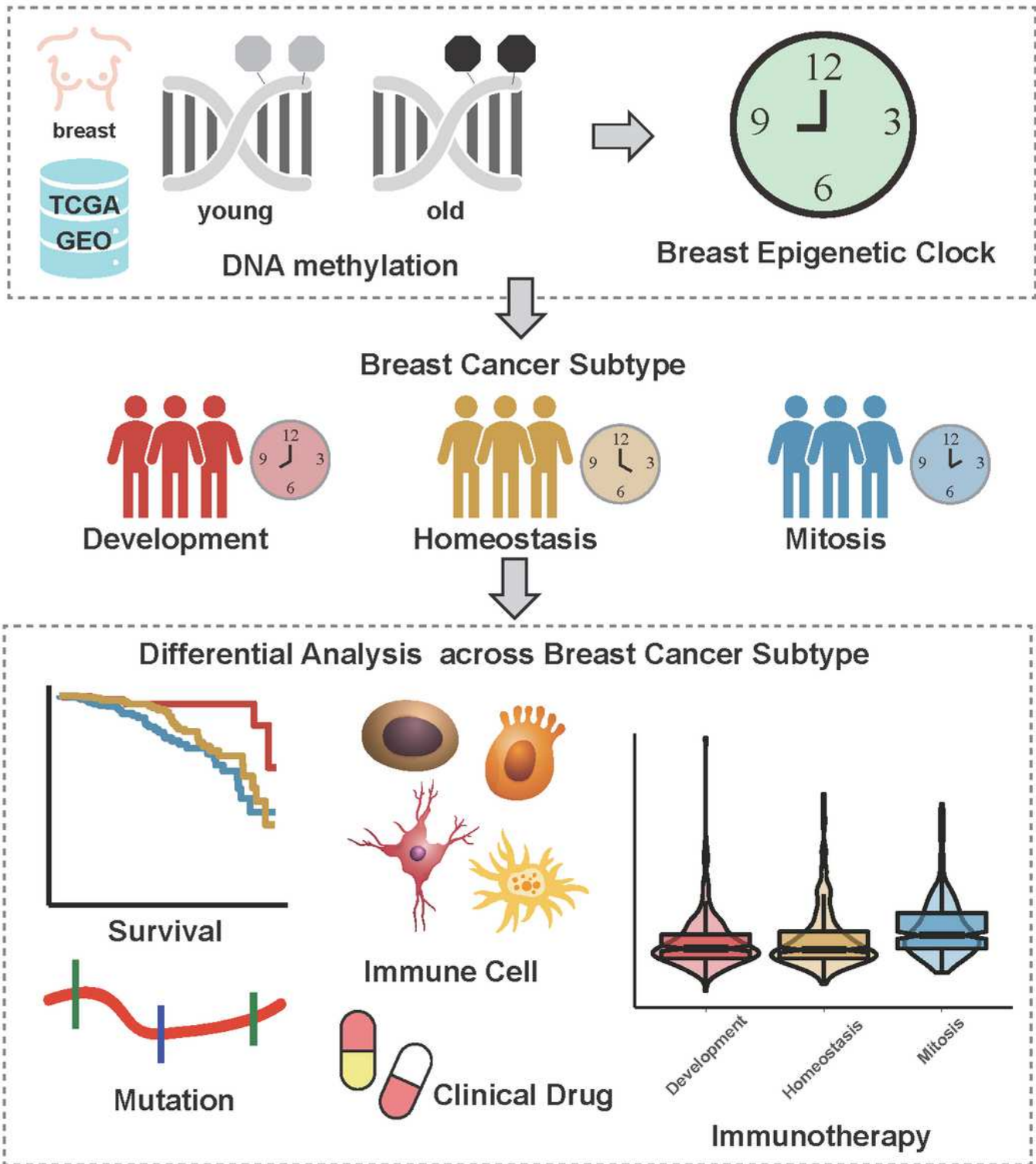


Figure 1

The Construction and application of breast epigenetic clock.

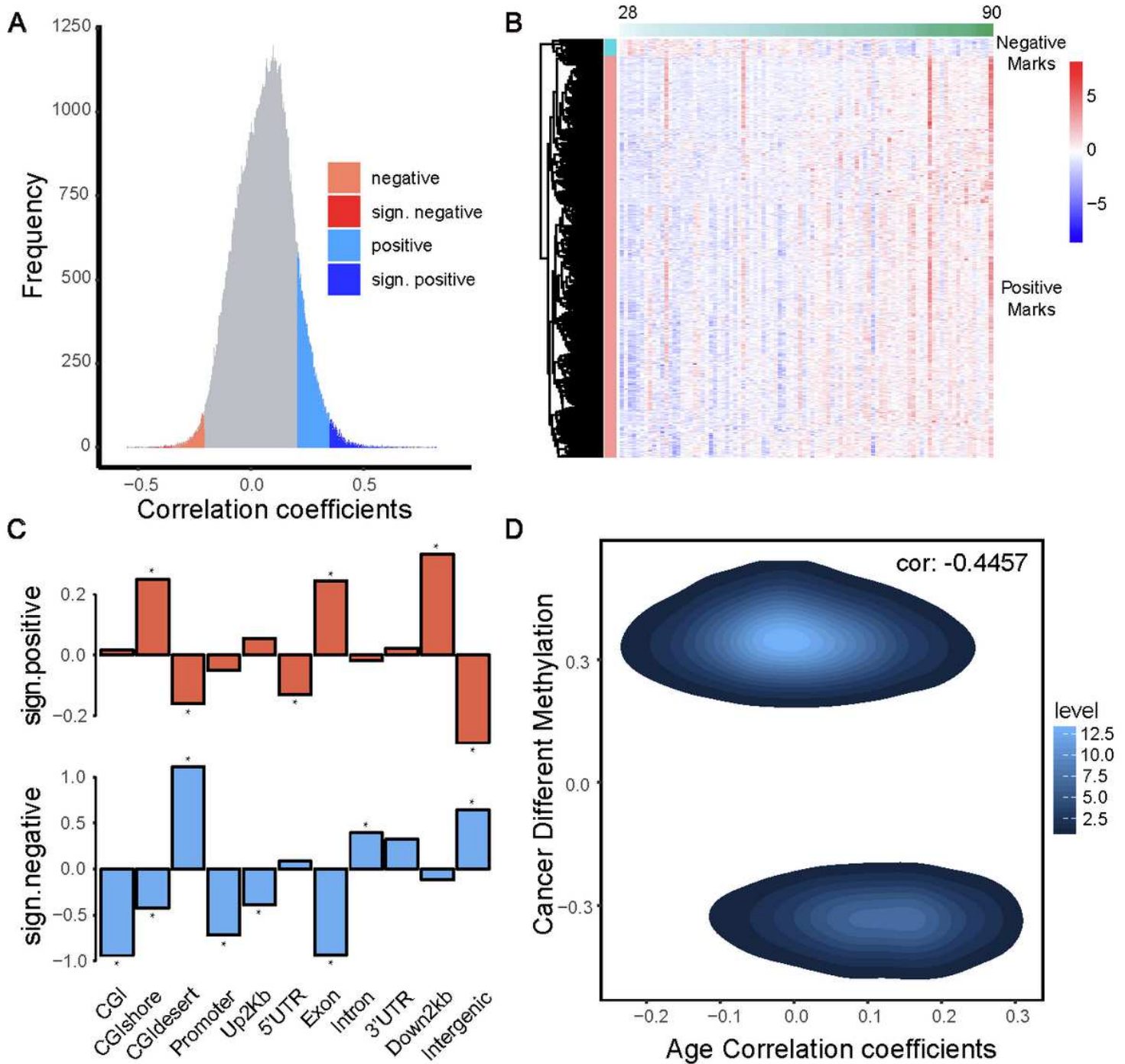


Figure 2

Aging-associated CpG sites in normal breast tissue. (A) Overview of Pearson correlation calculated in normal breast tissue. Nominal correlations are highlighted (p value < 0.05) in wathet (positive) and light red (negative). Significant correlations are highlighted (FDR < 0.05) in blue (positive) and red (negative). (B) Heatmap of DNA methylation of aging-associated CpG sites. A white to green gradient represents the gradual increase in age. (C) Genome enrichment of aging-associated CpG sites (tested using chi-square test; *p value < 0.05). (D) Correlation between DNA methylation difference of DMC and aging-correlation coefficient of DMC. The horizontal axis represents the correlation coefficient between age and DNA

methylation of DMC in normal samples. The vertical axis represents DNA methylation difference between cancer samples and normal samples.

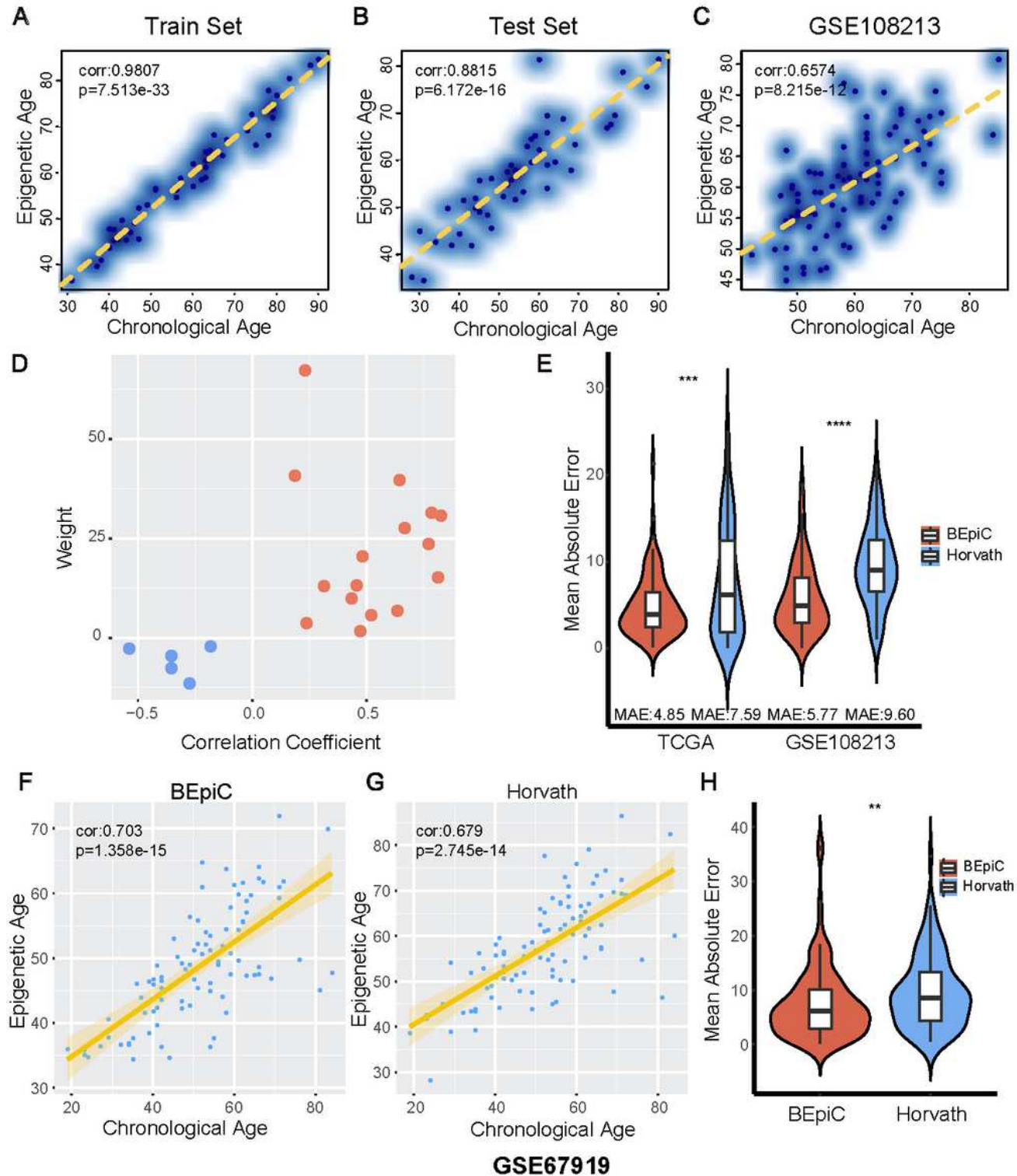


Figure 3

Chronological age was predicted based on DNA methylation in human breast tissue. (A-C) Epigenetic age vs. chronological age from training set (A), testing set (B) and GSE108213 dataset (C). (D) Scatter plot depicting the relationship between weight and aging-correlation coefficient of CpG sites. Blue spots are

negatively aging-associated CpG sites and orange spots are positively aging-associated CpG sites. (E) Comparison of predictive performance between BEpiC and the Horvath clock. The Y-axis represents the mean absolute error between epigenetic age and chronological age (tested using t test; * represent $p < 0.05$, ** represent $p < 0.01$, *** represent $p < 0.001$, **** represent $p < 0.0001$). (F-G) Chronological age vs. epigenetic age estimated by BEpiC (F) and Horvath clock (G) in GSE67919. (H) Comparison of predictive performance between BEpiC and the Horvath clock in GSE67919 (tested using t test; * represent $p < 0.05$, ** represent $p < 0.01$, *** represent $p < 0.001$, **** represent $p < 0.0001$).

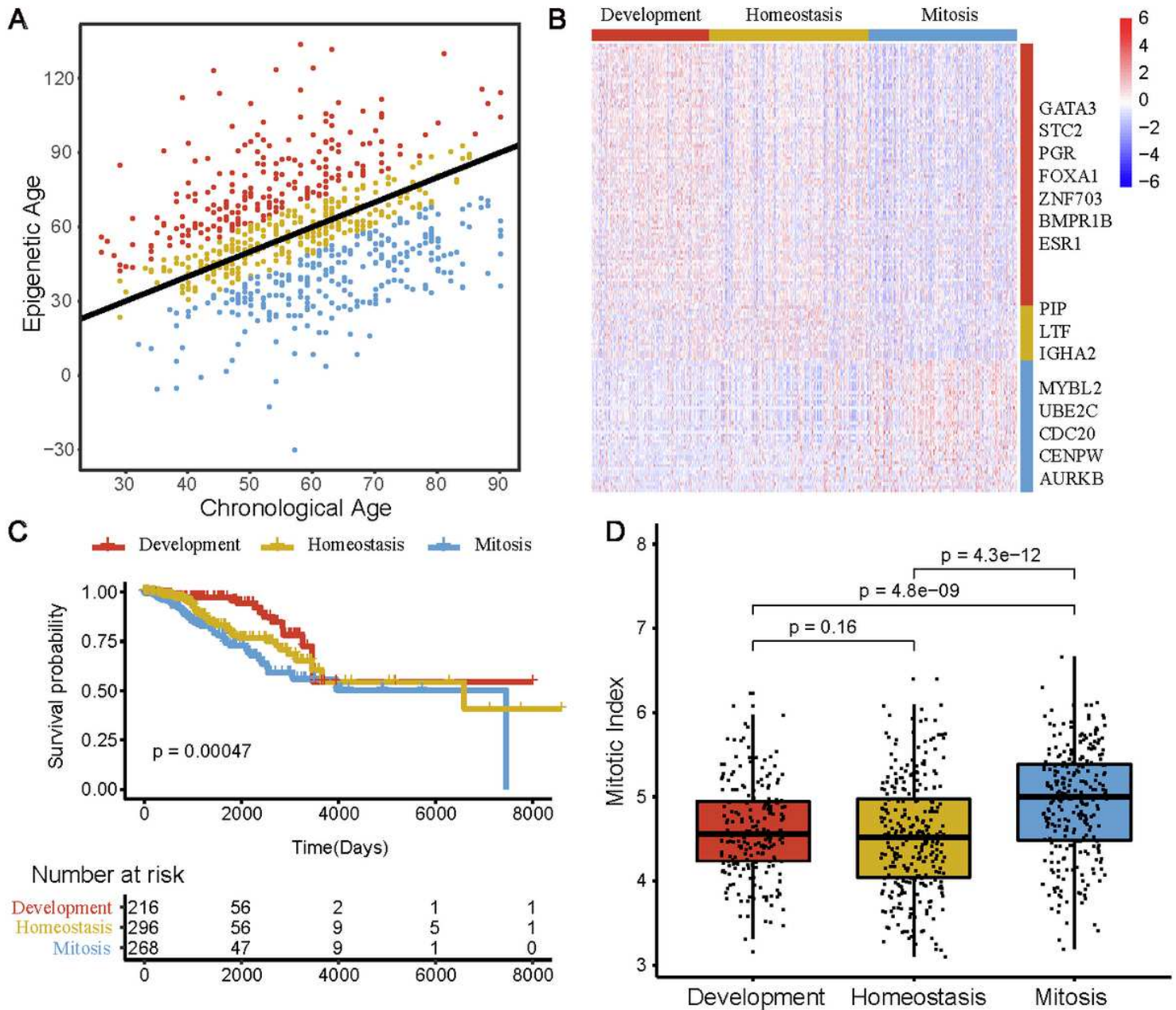


Figure 4

Three breast cancer subtypes identified by BEpiC based on epigenetic age. (A) Subtypes of breast cancer were classified based on the deviation between methylated age and chronological age. (B) Gene

signature expression profiler and GO annotation for the three subtypes. The red dot, the yellow dot, and the blue dot represent development subtype, homeostasis subtype and mitosis subtype, respectively. (C) Kaplan–Meier curve for patients of the three subtypes. (D) Mitotic index in three subtypes (p values by Wilcoxon test).

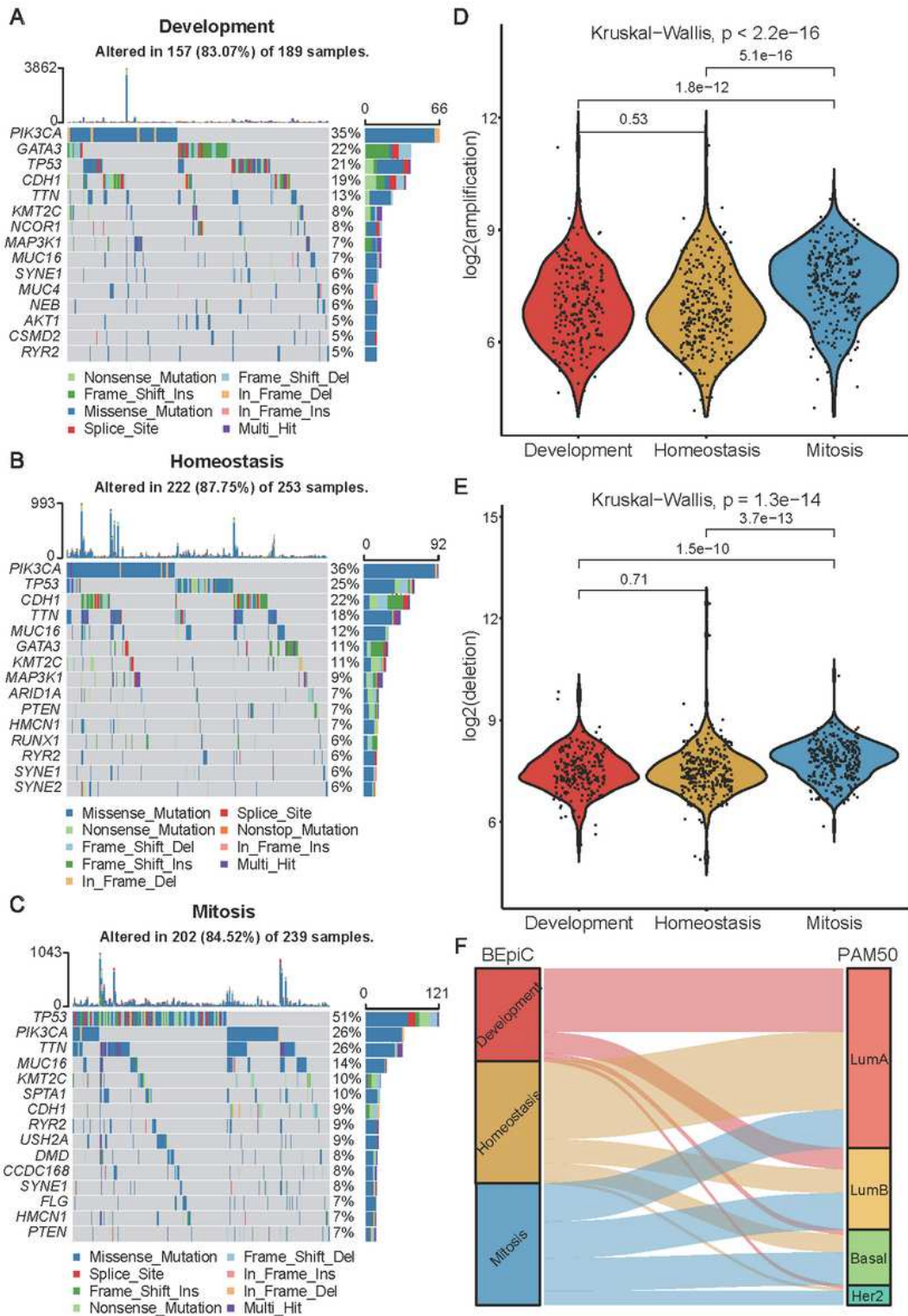


Figure 5

Molecular differences among the three subtypes. (A-C) Gene mutation frequency in development subtype (A), homeostasis subtype (B) and mitosis subtype (C). (D-E) Number of copy number amplification (D) and copy number deletion (E) among the three subtypes (P values by Kruskal-Wallis test). (F) Association between breast cancer subtypes defined by BEpiC and pam50 molecular subtypes.

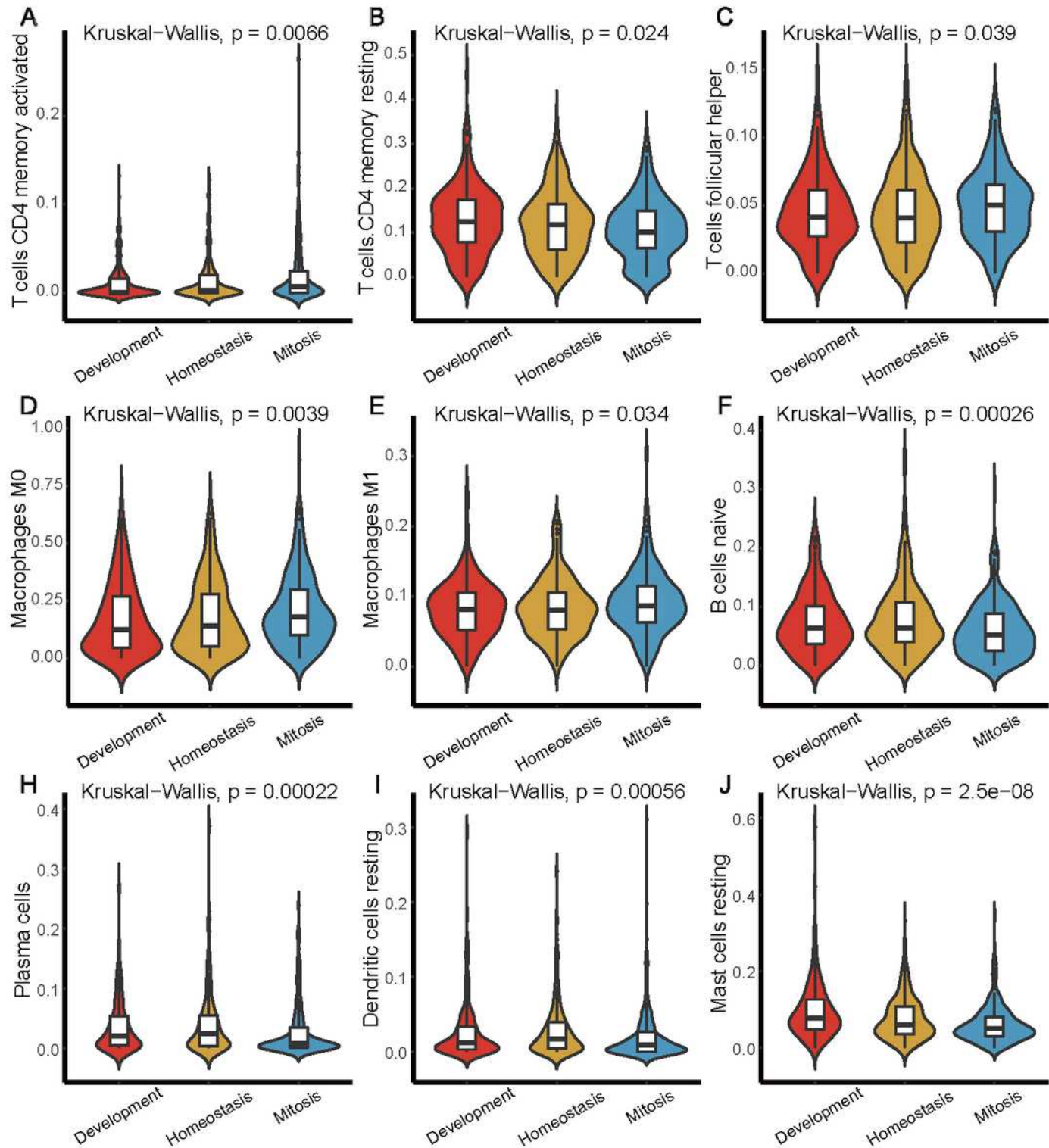


Figure 6

Immune infiltrating cells that differ significantly between the three subtypes. (A-J) Comparison of proportion of T cell CD4 memory activated, T cell CD4 memory resting, T cell follicular helper, Macrophages M0, Macrophages M1, B cells naive, Plasma cells, Dendritic resting, Mast cells resting among the three subtypes (P values by Kruskal-Wallis test).

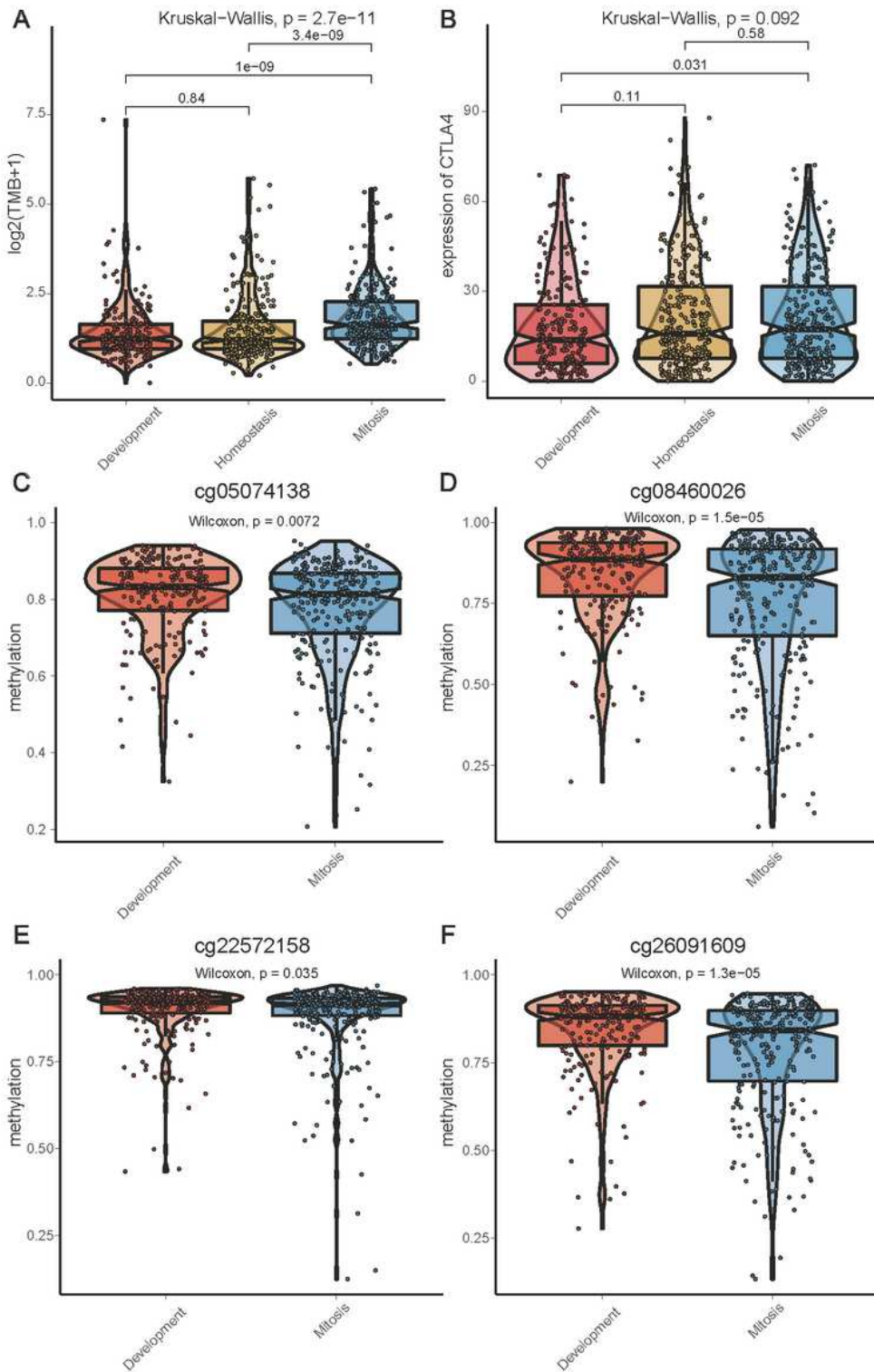


Figure 7

Comparison of immunotherapeutic response among the three subtypes. (A) Tumor mutation burden in each subtype (P values by Kruskal-Wallis test). (B) Expression of CTLA4 in each subtype (P values by Kruskal-Wallis test). (C-F) Methylation level of cg05074138 (C), cg08460026 (D), cg22572158 (E) and cg26091609 (F) in development subtype and mitosis subtype.

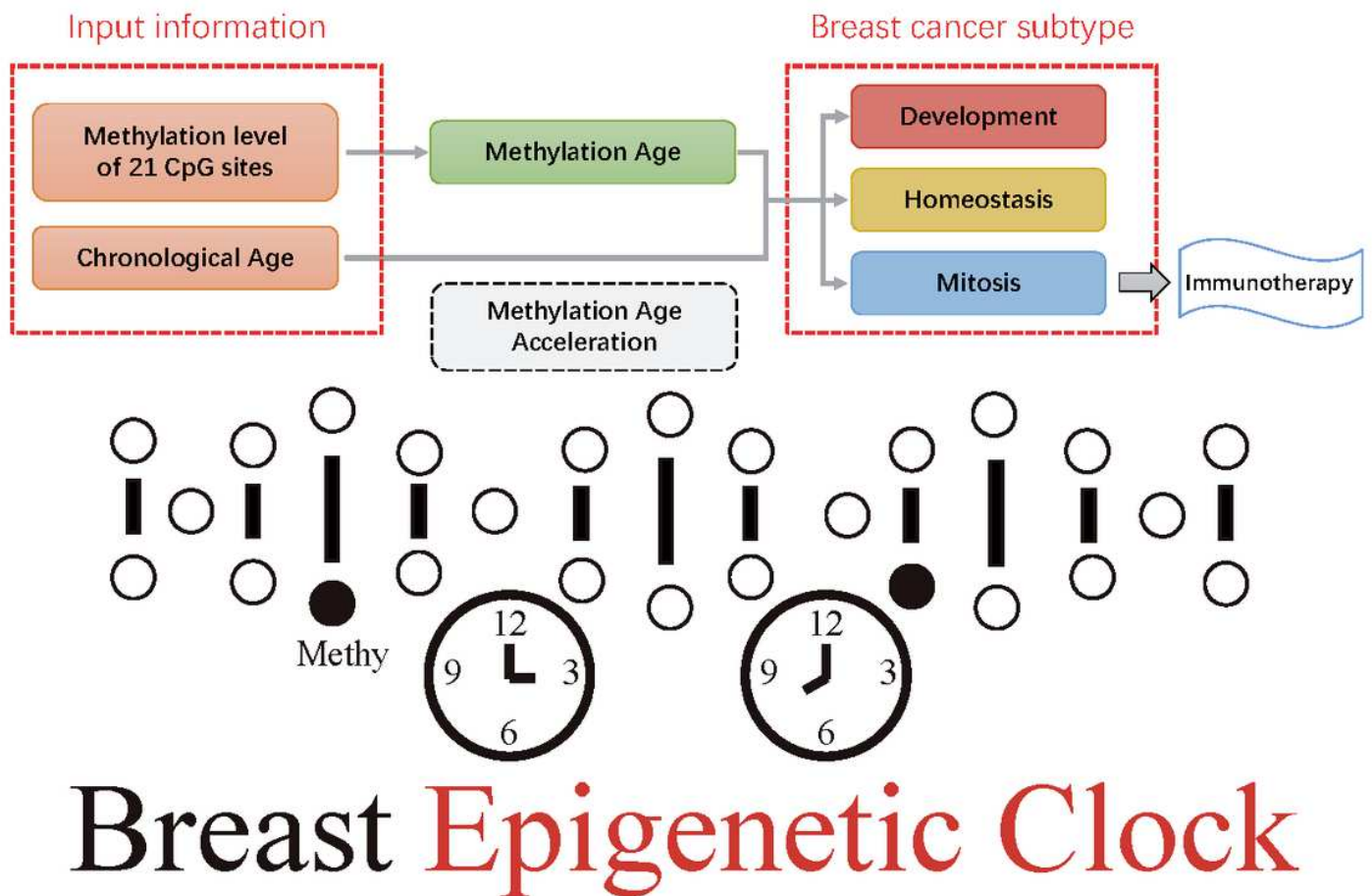


Figure 8

Schematic overview of the breast epigenetic clock. The web server could use the data submitted by the user to calculate the epigenetic age and breast cancer subtypes.

Supplementary Files

This is a list of supplementary files associated with this preprint. Click to download.

- [SupplementaryFigure1.pdf](#)
- [SupplementaryFigure2.pdf](#)
- [SupplementaryFigure3.pdf](#)
- [SupplementaryFigure4.pdf](#)
- [SupplementaryFigure5.pdf](#)

- [SupplementaryFigure6.pdf](#)
- [Supplementarymaterial.pdf](#)